Development 135, 1935-1946 (2008) doi:10.1242/dev.017160

The multidomain protein Brpf1 binds histones and is required for Hox gene expression and segmental identity

Kathrin Laue[1,*], Sylvain Daujat[2,*], Justin Gage Crump[3], Nikki Plaster[1,†], Henry H. Roehl[4], Tübingen 2000 Screen Consortium[‡], Charles B. Kimmel[5], Robert Schneider[2,§] and Matthias Hammerschmidt[1,6,§]

The Trithorax group (TrxG) is composed of diverse, evolutionary conserved proteins that form chromatin-associated complexes accounting for epigenetic transcriptional memory. However, the molecular mechanisms by which particular loci are marked for reactivation after mitosis are only partially understood. Here, based on genetic analyses in zebrafish, we identify the multidomain protein Brpf1 as a novel TrxG member with a central role during development. *brpf1* mutants display anterior transformations of pharyngeal arches due to progressive loss of anterior Hox gene expression. Brpf1 functions in association with the histone acetyltransferase Moz (Myst3), an interaction mediated by the N-terminal domain of Brpf1, and promotes histone acetylation in vivo. Brpf1 recruits Moz to distinct sites of active chromatin and remains at chromosomes during mitosis, mediated by direct histone binding of its bromodomain, which has a preference for acetylated histones, and its PWWP domain, which binds histones independently of their acetylation status. This is the first demonstration of histone binding for PWWP domains. Mutant analyses further show that the PWWP domain is absolutely essential for Brpf1 function in vivo. We conclude that Brpf1, coordinated by its particular set of domains, acts by multiple mechanisms to mediate Moz-dependent histone acetylation and to mark Hox genes for maintained expression throughout vertebrate development.

KEY WORDS: Brpf1, Bromodomain, PWWP domain, Moz, Hox gene expression, Craniofacial development, Cranial neural crest, Pharyngeal arch, Anterior-posterior patterning, Homeotic transformation, Zebrafish

INTRODUCTION

Anterior-posterior patterning of the vertebrate head, including segmental identity determination of the seven pharyngeal arches, is governed by differential Hox gene expression (reviewed by Santagati and Rijli, 2003). Chondrocytes of the arches derive from cranial neural crest (CNC) cells of the midbrain and hindbrain region (Le Douarin, 1982). CNC forming the first pharyngeal arch (mandibular) is devoid of Hox gene expression, whereas cells contributing to the second (hyoid) and posterior (branchial, gill) arches display a nested pattern of Hox gene expression (the 'Hox code') (Hunt et al., 1991) (reviewed by Santagati and Rijli, 2003). The most-anteriorly expressed Hox genes, *Hoxa2* in mouse and *hoxa2b* and *hoxb2a* in zebrafish, determine second arch identity. Ectopic expression of *hox2* in the first arch causes it to acquire second arch identity, resulting in two hyoids (Grammatopoulos et al., 2000; Hunter and Prince, 2002; Pasqualetti et al., 2000). Conversely, loss of *hox2* results in an anterior homeotic transformation of the second arch to first arch identity and a bimandibular phenotype (Gendron-Maguire et al., 1993; Hunter and Prince, 2002; Rijli et al., 1993). Interestingly, tissue-specific deletion of mouse *Hoxa2* in post-migratory neural crest cells reproduces the conventional knockout phenotype, demonstrating the requirement for maintained Hox expression in CNC (Santagati et al., 2005).

Maintenance of Hox gene expression is regulated by the antagonistic function of Polycomb group (PcG) and Trithorax group (TrxG) proteins. Many PcG and TrxG factors were identified in *Drosophila* by mutations that produce or suppress specific homeotic phenotypes in segment identity. They have been fairly well conserved throughout evolution. Most of them act in large complexes and modify the local properties of chromatin to maintain transcriptional repression (PcG) or activation (TrxG) of their target genes through the cell cycle, thereby accounting for epigenetic transcriptional memory (reviewed by Ringrose and Paro, 2004; Ringrose and Paro, 2007; Simon and Tamkun, 2002). Biochemically, the roles of the different TrxG proteins are diverse. Some members bind to particular cis-regulatory DNA sequences in their target genes [e.g. Polycomb/Trithorax response elements (PRE/TREs) in *Drosophila*], whereas others are involved in histone binding or enzymatic histone modification. Prominent examples are Trithorax itself and its mammalian orthologs, the Mll (Mixed-lineage leukemia) proteins, which are histone H3 lysine 4 (K4H3) methyltransferases (reviewed by Popovic and Zeleznik-Le, 2005). In *Mll1*-deficient mouse embryos, Hox gene expression is not properly maintained, leading to anterior homeotic transformations of segmental identities and defects during hematopoesis (Yagi et al., 1998; Yu et al., 1998; Yu et al., 1995). More recently, based on genetic analysis in zebrafish, a TrxG-like function required to maintain cranial Hox gene expression was assigned to Moz (Monocytic leukemia zinc-finger protein; Myst3 – ZFIN) (Miller et al., 2004), a histone acetyltransferase (HAT) of the MYST family, which in mouse is also required for maintenance of hematopoietic stem cells (Katsumoto et al., 2006; Thomas et al., 2006).

[1]Georges-Koehler-Laboratory and [2]Hans-Spemann-Laboratory, Max-Planck-Institute of Immunobiology, Stuebeweg 51, D-79108 Freiburg, Germany. [3]Center for Stem Cell and Regenerative Medicine, USC Keck School of Medicine, Los Angeles, CA 90033, USA. [4]Centre of Developmental and Biomedical Genetics, University of Sheffield, Sheffield S10 2TN, UK. [5]Institute of Neuroscience, 1254 University of Oregon, Eugene, OR, USA. [6]Institute for Developmental Biology, University of Cologne, D-50923 Cologne, Germany.

*These authors contributed equally to this work
[†]Present address: Department of Developmental and Cell Biology, UCI, Irvine, CA 92697, USA
[‡]A list of the members of the Consortium and their affiliations is provided at the end of the article
[§]Authors for correspondence (e-mail: schneiderr@immunbio.mpg.de; hammerschmid@immunbio.mpg.de)

Accepted 27 March 2008

Here, based on the positional cloning of bimandibular zebrafish mutants, we identify the multidomain protein Brpf1 (Bromodomain and PHD finger containing 1; also known as Br140 and Peregrin) as a TrxG member and close partner of Moz. Brpf1 contains a unique combination of domains typically found in chromatin-associated factors, including PHD fingers, a bromodomain and a PWWP domain. Bromodomains interact with acetylated lysines on N-terminal tails of histones and other proteins (reviewed by Yang, 2004), and PHD fingers were recently shown to bind to methylated K4H3 (Shi et al., 2006; Wysocka et al., 2006), whereas the histone-binding properties of PWWP domains remain to be shown. Based on its domains, Brpf1 has been proposed to be involved in chromatin remodeling (Thompson et al., 1994). However, its exact function in vertebrates is currently unknown.

In this study, we show that during zebrafish development, Brpf1 is required for histone acetylation, maintenance of cranial Hox gene expression and proper determination of pharyngeal segmental identities. We demonstrate genetic and physical interaction of Brpf1 with the HAT Moz. This interaction can explain how Brpf1 promotes histone acetylation. Furthermore, in contrast to Moz, Brpf1 remains associated with the chromatin even during metaphase, contributing to transcriptional memory throughout mitosis. We further show that the previously largely unappreciated PWWP domain is essential for histone binding and chromatin association of Brpf1 in interphase and mitosis, as well as for Brpf1 function in vivo. Together, these data identify Brpf1 as a novel TrxG protein with essential roles in epigenetic memory during vertebrate development.

MATERIALS AND METHODS

Zebrafish lines and genotyping

brpf1^{t20002} and *brpf1*^{t25114} alleles were obtained during the Tübingen 2000 screen at the Max-Planck Institute of Developmental Biology, *brpf1*^{b943} during a screen at the University of Oregon (Eugene, OR) (Miller et al., 2004). Unless stated otherwise, the *t20002* allele was used for phenotypic analyses. *brpf1*^{t20002} and *brpf1*^{b943} larvae were genotyped taking advantage of restriction fragment length polymorphisms. The *brpf1*^{t20002} mutation creates a *Dde*I restriction site, whereas *brpf1*^{b943} creates a *Tsp*45I site.

Genetic mapping and cloning of *brpf1*

For genetic mapping, carriers of the *brpf1*^{t20002} mutation were crossed to the polymorphic WIK line to generate hybrid F1 that were mated to each other. For rough mapping, PCR analysis of SSLP markers was carried out on genomic DNA pools of mutant F2 offspring or wild-type siblings (Geisler, 2002). For fine mapping with single F2 fish, new polymorphic markers were designed from genomic sequences identified by Blast searches. Marker KL001 from genomic fragment NA4876 with no recombination in 1800 meiosis was used to initiate a PCR-based chromosomal walk with the CHORIB736 BAC library (RZPD, Berlin, Germany). Genomic fragment NA8747 was isolated by Blast searches of the Ensembl database (http://www.ensembl.org) with end sequences of BAC zC105C2. It overlapped with NA5599, which contained three coding exons of zebrafish *brpf1*. Ensembl Zv6_scaffold1302 contains two non-coding and ten coding *brpf1* exons, whereas three additional coding exons were found in NCBI Whole Genome Shotgun (WGS) traces. Non-overlapping 5′ and 3′ zebrafish *brpf1* ESTs, fi61a03 and fe06c05, were identified by Blast searches of the zebrafish TGI database of the Gene Index Project (http://compbio.dfci.harvard.edu/tgi/tgipage.html) and the internal fragment was cloned by nested RT-PCR.

Morphological analysis and in situ hybridization

For the zebrafish *brpf1* in situ probe, pCRII-zfbrpf1 was linearized with *Acc*65I and transcribed with T7 RNA polymerase. Single and double in situ hybridization and immunostaining with α-MF20 (ZIRC; 1:100), α-GFP (Roche, 1:200) or α-p63 (4A4; Santa Cruz Biotechnology; 1:200) antibodies were performed as described (Hammerschmidt et al., 1996; Hauptmann and Gerster, 1994). For sectioning, stained larvae were embedded in JB4 plastic (Polysciences) and cut into 7-μm slices. Cartilage was stained with Alcian Blue and bone matrix with Alizarin Red, as described (Walker and Kimmel, 2007).

Morpholino and RNA injections, TSA treatment

Antisense morpholino oligonucleotides (MOs) were purchased from Gene Tools. Per embryo, 1.5 nl MO solution in Danieau's buffer were injected at the 1- to 2-cell stage. MO sequences and injected amounts were: *brpf1*, 5′-GTAAGTGCAGTACCTGTAGTAGCTC-3′ (1.5 ng); *moz*-MO3 (Miller et al., 2004) (1 ng). For synergistic enhancement experiments, 0.3 ng *moz* MO3 was co-injected with 0.5 ng *brpf1* MO. For RNA injections, capped mRNA was in vitro synthesized with the MessageMachine Kit (Ambion), and injected into 1- to 2-cell stage embryos (1.5 nl). Mouse *Brpf1* mRNA was prepared (*Cla*I/SP6) from pCMV-SPORT6 Brpf1 (RZPD), zebrafish *hoxb1a* mRNA from pCS2-hoxb1a (*Not*I/SP6) (McClintock et al., 2001). For rescue experiments, 0.1 ng RNA was injected per embryo. For Trichostatin A (TSA) treatment, dechorionated embryos were incubated in 250 nM TSA (Sigma) or DMSO (control) from 20-33 hpf.

Cell culture, co-immunoprecipitations, HAT assays and immunostaining

The mouse *Brpf1* fl clone (p998E1011925Q1, IMAGE ID 5363697) was obtained from RZPD and subcloned into the *Sma*I/*Xho*I sites of HA-pcDNA3 and pEGFP-C1 vectors (Invitrogen). Deletion constructs were generated by restriction digest and religation.

To examine the interaction of Brpf1 and Moz, HA- or GFP-Brpf1 expression constructs were transfected into HEK 293 cells along with the FLAG-Moz expression plasmid. Cells were lysed 48 hours post-transfection in buffer I (50 mM Tris-HCl pH 8, 150 mM NaCl, 0.75% Triton X-100, 0.1% NP40, protease inhibitors), extracts were affinity-purified with anti-FLAG M2 or anti-HA agarose beads (Sigma) and washed three times with buffer I. Bound proteins were separated on SDS-PAGE gels and transferred to nitrocellulose membrane, or used for HAT activity assays, which were performed as described (Bannister and Kouzarides, 1996) using purified human core histones.

For immunostaining, HEK 293 cells transfected with GFP-Brpf1 and/or FLAG-Moz expression plasmids were grown for 36 hours on poly-l-lysine-coated coverslips, fixed in 4% paraformaldehyde in PBS and permeabilized in 0.6% Triton X-100. Antibodies used were: H2AK5Ac (Abcam), H3K9me3 (Upstate), H3K4me1 (Abcam), H3K4me3 (Abcam), HA (Roche), FLAG (Sigma), GFP (Sigma), Moz (E-17, Santa Cruz), applied for 2 hours; Alexa-conjugated anti-mouse or anti-rabbit (488, 546 or 633 nm, Jackson ImmunoResearch), applied for 1 hour. After DNA counterstaining and mounting in Vectashield with DAPI (Vector Laboratories), cells were analyzed by confocal microscopy (Leica SP2). Metaphase chromosome spreads were carried out as described (Keohane et al., 1996).

Generation of recombinant protein and histone-binding assays

GST-Brpf1 domain fusions were expressed from pGEX2-TK plasmids in *Escherichia coli* (Rosetta Blue), and bound to Glutathione-Sepharose 4B beads according to the manufacturer's instructions (Amersham Biosciences). Core histones were acid-extracted from untreated or butyrate-treated HeLa cells, and 2 μg were incubated with bead-coupled GST fusion proteins for 3 hours at 4°C in 500 μl binding buffer (150 mM NaCl, 50 mM Tris-HCl pH 8, 50 mM $MgCl_2$, 0.25% NP40, 3% BSA, complete protease inhibitors). Beads were washed five times with binding buffer, resuspended in SDS sample buffer, and fractionated by 18% SDS-PAGE. Alternatively, 2 μg purified calf serum H2A or H2B histones (Roche) were used. Gels were stained with Coomassie Brilliant Blue (Sigma) or transferred to nitrocellulose for immunoblotting using anti-H2AK5Ac or anti-pan H2A primary antibodies (Upstate).

RESULTS

Zebrafish *brpf1* mutants display anterior shifts in segmental identities of pharyngeal arches 2-6

Zebrafish forward genetic screens after ENU mutagenesis and cartilage staining at 120 hours post-fertilization (hpf) yielded three non-complementing mutants (*t20002*, *t25114*, *b943*) with shifts in

segmental identities of craniofacial arches, but otherwise normal morphology (Fig. 1A,B). In wild-type larvae at 120 hpf (Fig. 1C), the ventral part of the first pharyngeal arch (Meckel's cartilage of mandibular) is characterized by the absence of a basal element, whereas such basal elements are present in arch 2 (basihyal of hyoid) and pharyngeal arches 3-7 (basibranchial of gill arches). In mutants, the basihyal was absent (Fig. 1D). In addition, both ventral and dorsal elements of arch 2 (ceratohyal and hyosymplectic) had shapes more similar to the corresponding elements of arch 1 (Meckel's cartilage and palatoquadrate) (Fig. 1C,D,J-L). An anterior transformation was also apparent with the molecular marker *bapx1* (*nkx3.2* – ZFIN), which in wild-type animals is exclusively expressed in joint cells between the ventral and dorsal element of arch 1 (Fig. 1M) (Miller et al., 2003), whereas mutants displayed ectopic *bapx1* expression in arch 2 (Fig. 1N). Corresponding anterior shifts also occurred for arch 2-associated muscles (Fig. 1O,P) and dermal bones, which were absent or strongly reduced in mutants (Fig. 1J,K,Q,R). Similarly, mutants lacked the specific ossification in both the dorsal and the ventral element of arch 2 (Fig. 1Q-T), leaving their central regions unossified as in arch 1. Furthermore, mutants displayed anterior transformations of pharyngeal arches 3-6 (gill arches), which acquired shapes and ossification patterns similar to arch 2 of wild-type animals (Fig. 1F-I,S,T).

Using meiotic segregation analysis, we mapped the *t20002* mutation within a 0.1 cM interval of chromosome 8 (Fig. 1U). Subsequent chromosomal walking led to the identification of a genomic fragment that contained sequences with high similarity to the mammalian bromodomain and PHD finger containing 1 (*Brpf1*) gene (see Materials and methods). The predicted protein of the full-length cDNA (3777 bp; GenBank accession number EU486162) is 71.4 and 71.1% identical with human and mouse Brpf1, respectively. Similarity is even higher within the conserved domains (C_2H_2 zinc finger, PHD, bromo and PWWP; see Fig. 1V), indicating that it is a true zebrafish Brpf1 ortholog. We identified molecular lesions in the *brpf1* gene of all three mutant alleles (Fig. 1V). *brpf1*^{t20002} contains a C135A transversion (see Fig. S1A in the supplementary material), introducing a TAA stop codon that leads to premature termination of the protein within the N-terminal C_2H_2 zinc finger. In the *brpf1*^{b943} allele, a G1044A transition introduces a TGA stop codon, resulting in a truncation of the protein within the PHD-finger domain. Finally, in *brpf1*^{t25114}, a T→A transversion creates a new intronic splice acceptor site 10 bp from the regular site at nucleotide position 2463 (see Fig. S1B in the supplementary material). This new splice site is preferentially used. Thus, 50/50 independent cDNA clones contained the corresponding 10 bp insertion that results in a frame shift and premature termination of the protein directly upstream of the C-terminal PWWP domain.

Strikingly, comparative analyses revealed that the phenotype of *t25114* mutants with the loss of the PWWP domain only, was at least as strong as that of the severely truncated and putative *brpf1*-null allele *t20002* (Table 1; see Fig. S1F-I in the supplementary material). Whole-mount in situ hybridizations (see Fig. S1C in the supplementary material) and semi-quantitative RT-PCR (see Fig. S1D in the supplementary material) further showed that the *t25114* mutation did not affect *brpf1* transcript stability, and t25114-truncated GFP-Brpf1 fusion protein was as stable as the full-length version (see Fig. S1E in the supplementary material). Together, this points to a pivotal role of the PWWP domain for proper Brpf1 function in vivo.

To provide further evidence for the causative nature of the identified *brpf1* mutations, we knocked down zygotic *Brpf1* in wild-type embryos by injection of antisense morpholino oligonucleotides (MOs) targeting the splice donor site between exon 1 and intron 1 (see Fig. S1J in the supplementary material). Morphant embryos displayed a complete loss of wild-type *brpf1* transcripts, as determined by semi-quantitative RT-PCR (see Fig. S1K in the supplementary material) and northern blotting (see Fig. S1L in the supplementary material), and displayed craniofacial defects indistinguishable from those of the mutants (Fig. 1D,E). Finally, zebrafish *brpf1* mutants injected with mouse *Brpf1* mRNA displayed a partial, but significant rescue of anterior Hox gene expression at 33 hpf (Fig. 2, compare I-L with E-H).

Table 1. Quantification of skeletal alterations of the three *brpf1* alleles and of *brpf1* morphants

	Percentage of animals with each phenotypic trait			
Skeletal alteration	*t20002*	*t25114*	*b943*	*brpf1* MO
Arch 2 (hyoid), ventral elements				
Basihyal absent	91	95	100	79
Basihyal reduced	9	5	0	21
Ceratohyal inversion	3	9	14	6
Ceratohyal shape change	44	72	100	97
Shorter	44	72	100	97
Broader	44	72	100	79
Distal ends bifurcated	35	72	100	79
Fusion ceratohyal-Meckel's cartilage	0	0	25	9
Arch 2 (hyoid), dorsal elements				
Hyosymplectic shape change	32	82	100	100
Symplectic extension shortened	32	82	79	91
Hyomandibular reduction (dorsal of foramen)	26	32	79	91
Fusion hyosymplectic-palatoquadrate	6	9	4	0
Arches 3-6				
Hyobranchials absent	100	100	100	79
Ceratobranchials distally broadened	55	95	100	48
Total number of animals examined	34 (100%)	22 (100%)	28 (100%)	33 (100%)

Skeletal alterations were assessed by Alcian Blue staining at 120 hpf (compare with Fig. S1F-H in the supplementary material). If anything, the *t25114* and *b943* alleles, which encode less severely truncated Brpf1 proteins, display slightly stronger, rather than weaker, phenotypes than the potential null allele *t20002*. For details, see text and Fig. 1. These subtle differences in phenotypic strengths are most likely due to differences in the genetic backgrounds.

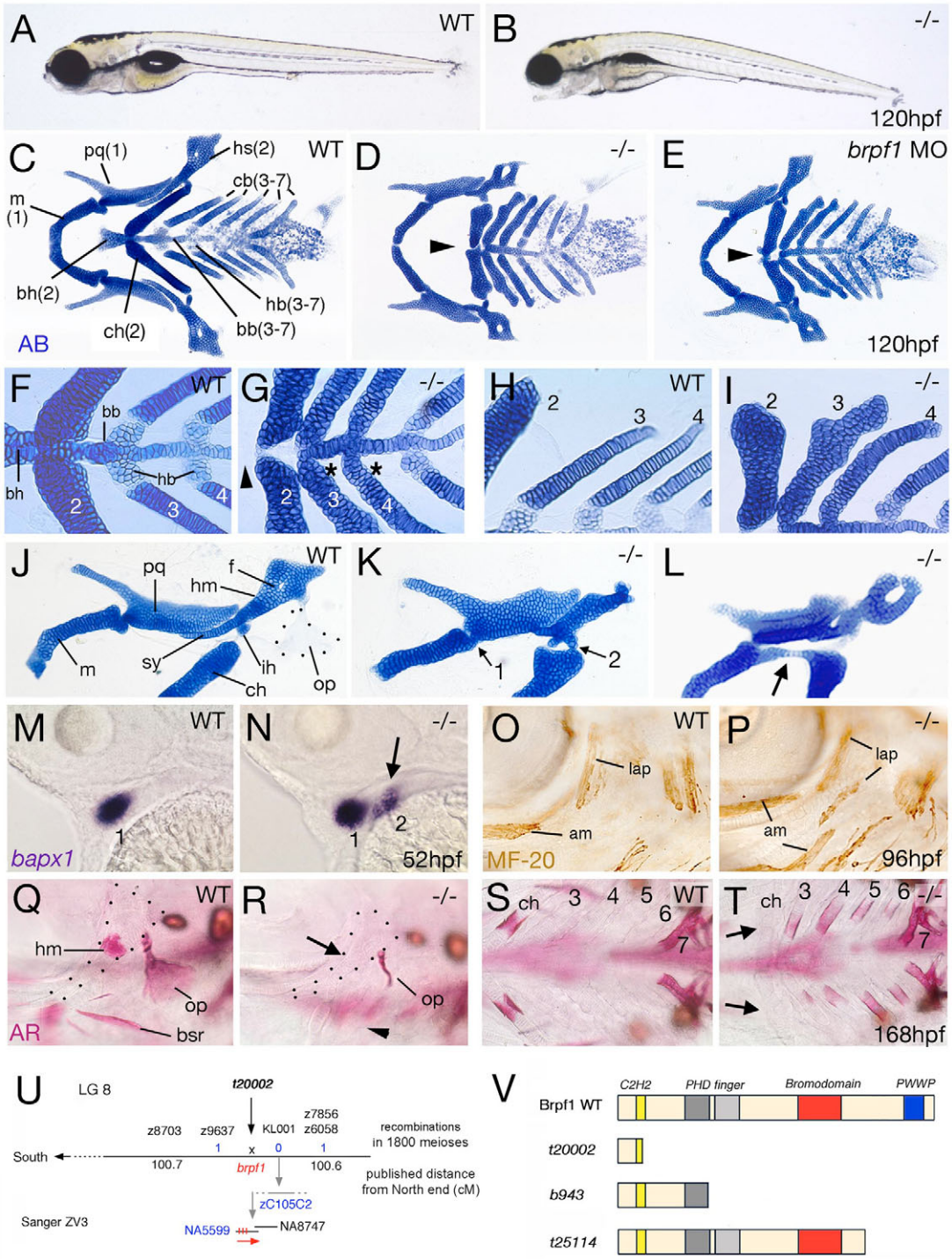

Fig. 1. See next page for legend.

Altogether, the data indicate that Brpf1 is absolutely essential for segmental pharyngeal identity, and that the functionality of Brpf1 has been conserved between zebrafish and mouse.

brpf1 is required for maintenance of cranial Hox gene expression

Anterior-posterior patterning of the vertebrate head, including the determination of pharyngeal arch identity, is governed by differential Hox gene expression (Santagati and Rijli, 2003). Therefore, we studied whether Brpf1 might act upstream of Hox genes. CNC cells contributing to arch 1 cartilage lack Hox gene expression, whereas cells contributing to arch 2 display expression of *hoxa2b* and *hoxb2a*, and cells contributing to arches 3-7 display expression of *hoxa2b* and *hoxb3a* (Fig. 2B-D) (Hunter and Prince, 2002). In *brpf1* mutants, expression of all Hox genes in hindbrain and CNC was initiated normally during segmentation stages (see Fig. S2 in the supplementary material). However, at 26 hpf (data not shown) and 35 hpf, CNC expression of *hoxa2b* and *hoxb2a* was completely absent in mutant embryos (Fig. 2F,G). *hoxb3a* transcripts were only lost in the anterior, being present at reduced levels in the posterior CNC (Fig.

Fig. 1. Zebrafish *brpf1* mutants display anterior shifts in pharyngeal arch identities. Genotypes of fish are indicated in upper right corners (WT, wild type; –/–, homozygous *brpf1* mutant; MO, *brpf1* morphant), stages in lower right corners. (**A**,**B**) Lateral views of live larvae. (**C-L**) Cartilaginous elements of visceral skeleton stained with Alcian Blue (AB). (C-I) Ventral views; neurocranium has been removed. Numbers of pharyngeal arches are indicated (1-7). Arrowheads (D,E,G) point to absent basihyal (bh) of mutant arch 2. In addition, arches 3 and 4 of the *brpf1* mutant lack hypobranchials (hb) (G, asterisks), intermediate elements that (in wild-type larvae) are characteristic for arches 3-7, but absent in arches 1 and 2 (C,F). Furthermore, the distal ends of the mutant ceratobranchials (cb) (I; 3,4) have acquired the shape and organization of the ceratohyal (ch) of the second arch of wild-type larvae (H; 2). (J-L) Lateral views of arches 1 and 2. Arrows in K point to joints between ventral and dorsal elements (compare with N). Arrow in L points to fusion between Meckel's cartilage (m) of arch 1 and the transformed ceratohyal (ch) of arch 2, an ultimate sign of segmental identity. Note the variable loss of cartilage dorsal of the foramen (f) (K,L), the reduction of the symplectic extension (sy) of the transformed hyosymplectic (hs) and its fusion with the interhyal (ih) (K), which is an arch 2-specific linker element absent in arch 1 (J), giving the hyosymplectic a spatial organization more similar to that of the palatoquadrate (pq). (**M**,**N**) Lateral views of head region ventral to eyes after in situ hybridization for *bapx1*, a first arch joint marker. Arrow points to ectopic *bapx1* expression in arch 2 of the *brpf1* mutant. (**O**,**P**) Lateral views of head region posterior to eyes after immunostaining of pharyngeal muscles with anti-MF20 antibody. (**Q-T**) Lateral (Q,R) and ventral (S,T) views of heads after staining of bone matrix with Alizarin Red (AR). Arrows point to absent ossification in ceratohyal (ch, ventral element; R) and hyomandibula (hm, dorsal element; T) of arch 2 in the mutant. In addition, the branchiostegal rays (bsr) and the opercle (op) dermal bones associated with the ventral and dorsal element of arch 2, respectively, are absent (arrowhead in R) or reduced. Furthermore, ceratobranchials (cb) of arches 3-6 display ectopic central ossifications (T), as in the wild-type ceratohyal of arch 2 (S). By contrast, arch 7 appears normal (S,T), with characteristic pharyngeal teeth formation (Van der Heyden et al., 2001). (**U**) Genetic and physical map of the *t20002* allele of zebrafish *brpf1*. The three *brpf1* exons on genomic fragment NA5599 are indicated in red. (**V**) Schematic of predicted wild-type and *t20002*, *b943* and *t25114* mutant Brpf1 proteins, with the C_2H_2, PHD finger, bromo and PWWP domains in different colors. am, adductor mandibulae; bb, basibranchial; ih, interhyal; lap, levator arcus palatini.

2H), whereas expression of the more-posterior Hox genes (*hoxb6b*, *b7a*, *b8a*, *b9a*) was unaffected (data not shown). However, CNC cells displayed normal migration patterns, as revealed by *dlx2a* in situ hybridizations (Akimenko et al., 1994) (data not shown). We conclude that Brpf1 is specifically required for the maintenance, but not for the initiation, of anterior Hox gene expression. Interestingly, in the hindbrain, effects of *brpf1* mutations on *hox2* and *hox3* expression maintenance (Fig. 2G,H and see Fig. S2F in the supplementary material) were less severe than in the CNC. This suggests that Brpf1 function in the hindbrain is less crucial than that in the CNC, consistent with our findings that hindbrain patterning in *brpf1* mutants is largely normal (see Fig. S4A-D in the supplementary material).

The *brpf1* mutant phenotype is partially rescued by forced expression of *hox2* genes

To address whether the reduction of Hox gene expression is causative of the later pharyngeal segmental defects of *brpf1* mutants, we tried to rescue the bimandibular phenotype by reintroducing *hox*2 transcripts. Ectopic *hox2* gene expression during early segmentation stages can be obtained by injecting *hoxb1a* mRNA at the 1-cell stage (Hunter and Prince, 2002). *hoxb1a* RNA-injected wild-type embryos displayed a transformation of first to second arch identity, characterized by the loss of *bapx1* expression (Fig. 2O). The same effect was observed upon injection into *brpf1* mutants (Fig. 2, compare left side of P with N), indicating a conversion of the bimandibular to a bihyoid phenotype. Alternatively, injected mutants showed a particular reduction of ectopic *bapx1* expression in the second arch, resembling the wild-type situation (Fig. 2, compare right side of P with M). We conclude that Brpf1 regulates segmental identity of pharyngeal arches via its positive effect on Hox gene expression.

brpf1 is expressed in different craniofacial cell types and promotes Hox gene expression in a cell-autonomous fashion

Anterior Hox genes are expressed in hindbrain, CNC and pharyngeal endoderm and ectoderm (Crump et al., 2006). *brpf1* displayed transient expression in all of these cell types. During blastula, gastrula and early segmentation stages, it was uniformly expressed throughout the entire embryo (see Fig. S3A-C in the supplementary material; 0-11 hpf), whereas during mid-segmentation stages, *brpf1* expression was largely confined to the anterior half of the embryo (see Fig. S3D in the supplementary material; 17 hpf). At 26 hpf, strong expression was observed in brain, eyes, post-migratory CNC and pharyngeal endoderm (Fig. 3A-D). However, at 55 hpf, *brpf1* expression in specifying chondrocytes and endodermal pouches of the pharyngeal arches had largely ceased, while expression was maintained in pharyngeal and oral ectoderm (Fig. 3E-I). Strong and persistent *brpf1* expression could also be detected in brain and retina, and in the gastrointestinal tract, including liver and pancreas (see Fig. S3E-K in the supplementary material).

Studies with chimeric embryos showed that Brpf1 regulates Hox expression both in CNC (*hoxa2b*; Fig. 3J-O) and hindbrain (*hoxb1a*; see Fig. S4E-H in the supplementary material) in a cell-autonomous manner, indicating that the effect is direct and is not mediated via secreted posteriorizing signals. Chimeric studies with transplanted cells exclusively in the endoderm further revealed that Brpf1 expression in the pharyngeal endoderm is neither necessary nor sufficient for segmental identity of pharyngeal arches (see Fig. S5 in the supplementary material), pointing to a direct effect in the CNC.

Brpf1 genetically interacts with the HAT Moz, and the *brpf1* mutant phenotype is rescued by HDAC inactivation

A pharyngeal segmental identity phenotype very similar to that of *brpf1* mutants has been reported for zebrafish mutants in Moz, a transcriptional coactivator and HAT of the MYST family (Crump et al., 2006; Miller et al., 2004). Upon co-injection of sub-optimal amounts of *brpf1* and *moz* MOs, which upon single injections did not produce any apparent phenotype, we obtained reduced *hox2* gene expression (Fig. 4A-D, n=25/25; see Fig. S6A-D in the supplementary material, n=15/16) and pharyngeal identity defects as severe as in the strongest *brpf1* or *moz* morphants (Fig. 4E-H, n=15/15; see Fig. S6E-H in the supplementary material, n=12/12). This indicates that partial loss of Brpf1 activity synergistically enhances the effects caused by partial loss of Moz activity and vice versa. By contrast, *brpf1* mutants injected with the highest amounts

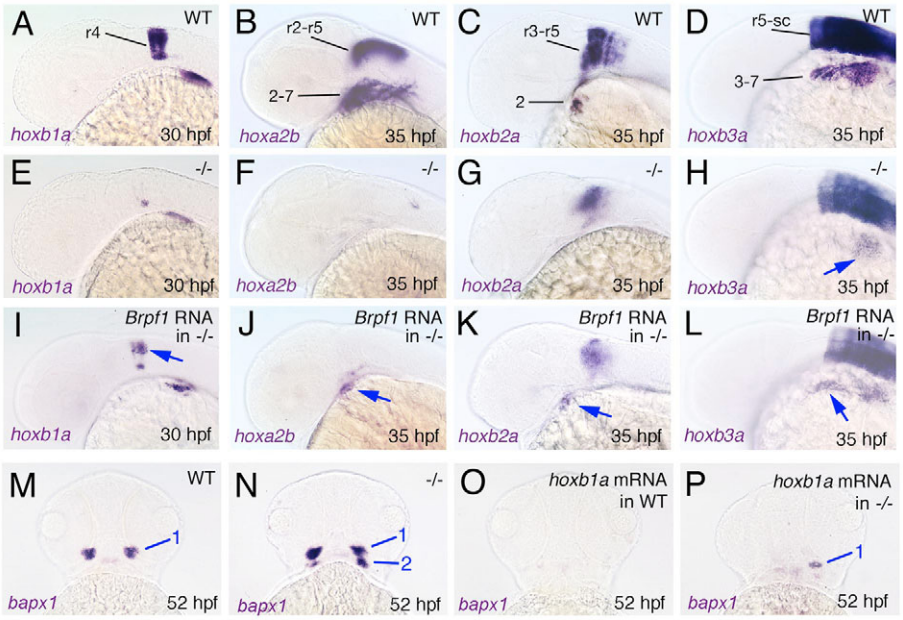

Fig. 2. Brpf1 regulates segmental identity by maintaining anterior Hox gene expression. Whole-mount in situ hybridizations with the probes indicated bottom left at the stages indicated bottom right; genotypes and treatment of zebrafish embryos as indicated in upper right corners. (A-L) Lateral views; (M-P) ventral views. (**A-D**) Hox gene expression in wild type (WT). Hox-expressing hindbrain rhombomeres (r) and arch-forming cranial neural crest (CNC) (2-7) are indicated. sc, spinal cord. (**E-H**) Absent or reduced Hox gene expression in *brpf1* mutants (–/–). Arrow in H indicates the remaining *hoxb3a* expression in the posterior CNC. (**I-L**) Partially rescued Hox gene expression in the hindbrain (I, arrow) and the CNC (J-L, arrows) of *brpf1* mutants injected with mouse *Brpf1* mRNA. (**M-P**) The bimandibular phenotype of the *brpf1* mutant (N) can be overcome by injection of *hoxb1a* mRNA. (O) *hoxb1a*-injected wild-type embryo lacking *bapx1* expression, indicative for bihyoid phenotype [compare with Hunter and Prince (Hunter and Prince, 2002)]. (P) *hoxb1a*-injected *brpf1* mutant with bihyoid pattern on left side and wild-type pattern on right side. Arch numbers are indicated.

moz MOs showed a phenotype no more severe than that of *moz* single morphants (see Fig. S6I,J in the supplementary material, *n*=23/23).

Moz is a HAT, suggesting that the segmental defects of *brpf1* mutants might be due to histone hypoacetylation. To test this, we treated *brpf1* mutants with the histone deacetylase (HDAC) inhibitor Trichostatin A (TSA). Treatment of mutants from 20-33 hpf rescued *hoxa2b* expression in CNC (Fig. 4I-L, *n*=9/9) and *hoxb1a* expression in the hindbrain (see Fig. S6K-N in the supplementary material, *n*=13/13) to wild-type levels, and led to a significant alleviation of skeletal defects at 120 hpf (see Fig. S6O-R in the supplementary material). Together, this suggests that Brpf1 and Moz tightly cooperate to determine pharyngeal segmental identities by promoting histone acetylation and maintenance of anterior Hox gene expression.

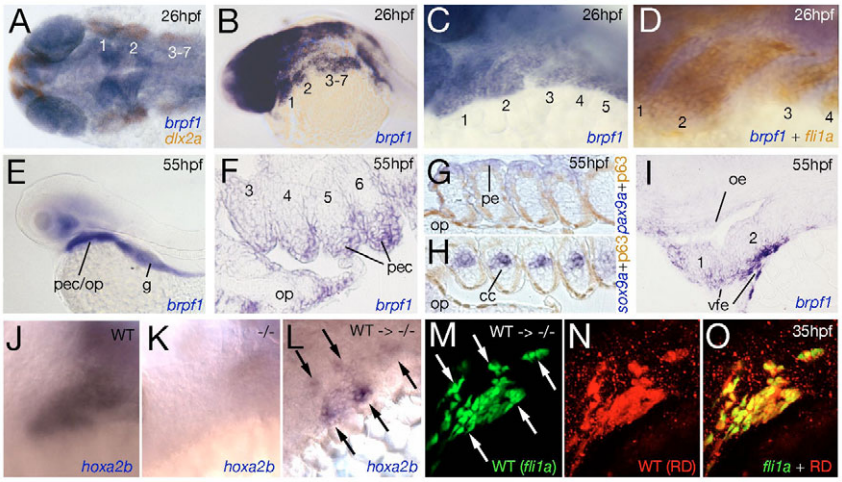

Fig. 3. Expression pattern and cell-autonomous function of *brpf1* in zebrafish CNC. Staining with reagents indicated at lower right at the stages indicated upper right. Numbers of pharyngeal arches are indicated (1-7). (**A-J**) Wild-type embryos; (**K**) *brpf1*^{b943} mutant (–/–); (**L-O**) mutant transplanted with wild-type cells (WT → –/–). (A) Dorsal view; (B-E,J-O) lateral views; (F-H) horizontal section; (I) longitudinal section. (A-D) At 26 hpf, *brpf1* is co-expressed with the CNC marker *dlx2a* (A) and with *fli1a* (D), stained by anti-GFP immunostaining of *tg(fli1a:EGFP)* embryo (Isogai et al., 2003). *brpf1*-positive cells between CNC include pharyngeal endoderm [D; compare with Fig. 1A in Crump et al. (Crump et al., 2004)]. (E-I) At 55 hpf, *sox9a*-positive chondrocytes of cartilage condensates (cc; H) (Yan et al., 2002) and *pax9a*-positive pharyngeal endodermal cells (pe; G) (Nornes et al., 1996; Okabe and Graham, 2004) lack *brpf1* expression, which, however, is strongly expressed in p63 (*tp63* – ZFIN)-positive cells (Carney et al., 2007) of the pharyngeal ectoderm (pec; F-H), in the oral ectoderm (oe; I) and in facial ectoderm ventral to arches 1 and 2 (vfe; I) (Crump et al., 2006). (J-O) Analysis of chimeric embryos with rhodamine-dextran (RD)-labeled (N) and *tg(fli1a:EGFP)*-positive (M) wild-type cells integrated in the CNC of a *brpf1* mutant host [for procedure, see Crump et al. (Crump et al., 2006)]. Only wild-type, not adjacent mutant CNC, cells display *hoxa2b* expression (arrows in L and M; *n*=3/3). g, gut; op, opercle.

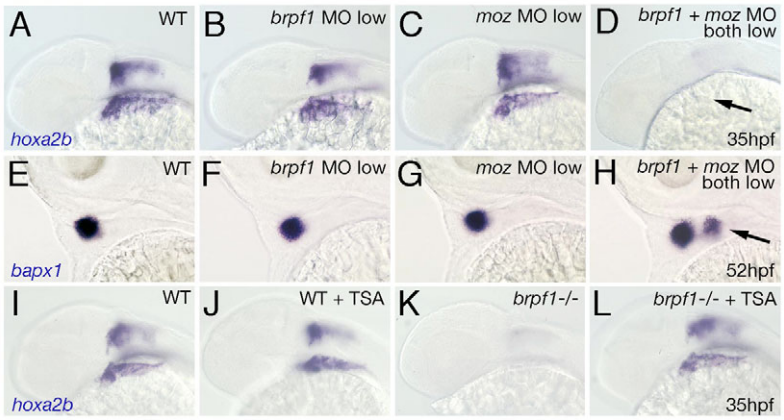

Fig. 4. Genetic interaction of Brpf1 and Moz and rescue of the *brpf1* mutant phenotype by TSA treatment. (**A-H**) Synergistic enhancement of phenotypes caused by partial loss of Brpf1 and Moz. *hoxa2b* (A-D; 35 hpf) and *bapx1* (E-H; 52 hpf) in situ hybridizations of zebrafish larvae after single or double injections of low amounts of MOs, as indicated in upper right corners. Lateral views. Arrow in D points to absent *hoxa2b* expression in CNC. Arrow in H indicates ectopic *bapx1* expression domain in arch 2. (**I-L**) Rescued *hoxa2b* expression in the *brpf1* mutant (–/–) after TSA treatment (compare L with K), whereas expression in treated wild-type siblings remains largely unaltered (compare J with I).

Brpf1 co-localizes and physically interacts with Moz

To examine and compare the subcellular localization of Brpf1 and Moz proteins, we transfected HEK 293 cells with expression constructs for GFP- or HA-tagged full-length Brpf1 and FLAG-tagged Moz. Immunofluorescence analyses revealed that Brpf1 and Moz co-localized in a specific punctate pattern in interphase nuclei (Fig. 5A). These domains most likely represent active chromatin, as indicated by co-localization with active histone marks (H2AK5Ac, H3K4me1, H3K4me3) and exclusion from regions with inactive marks (H3K9me3), both in interphase (data not shown) and during mitosis (Fig. 6I-K).

Reciprocal co-immunoprecipitations (Co-IP) with protein extracts of transfected HEK 293 cells further revealed that Brpf1 and Moz undergo (direct or indirect) physical association (Fig. 5G, upper panels). Importantly, the Brpf1-associated HAT activity towards histones H3 and H2A was similar to the specificity of immunoprecipitated Moz (Fig. 5G, bottom panels, lanes 3 and 7). A Moz-G657E mutant lacking HAT activity (Collins et al., 2006) was still able to associate with Brpf1, whereas only very little Brpf1-associated HAT activity could be detected (Fig. 5G, bottom panels, lanes 4 and 8). This indicates that Moz is the major HAT associated with Brpf1 and that its HAT activity is not required for the interaction with Brpf1. Confirming this, neither the co-localization with Brpf1 nor chromatin association required the HAT activity of Moz (Fig. 5B).

To map the Moz-interaction site of Brpf1, we carried out Co-IPs and co-localization experiments with a series of deletion or mutant constructs (Fig. 5F). These revealed that the N-terminal 245 aa containing the C_2H_2 zinc finger are necessary and sufficient for co-localization (Fig. 5C,D) and physical interaction with Moz (Fig. 5H, lanes 3, 6). The C_2H_2 zinc finger does not mediate this interaction, as mutant versions of it still interacted with Moz (Fig. 5I, lanes 5, 6), whereas an N-terminal 149 aa fragment with the intact zinc finger did not (Fig. 5I, lane 4), narrowing the interaction domain to a region between aa 150 and 245. Interestingly, the N-terminal 245 aa fragment of Brpf1, although sufficient for Moz co-localization, lost the typical punctate distribution in interphase nuclei (Fig. 5D). This suggests that the more C-terminal domains of Brpf1 are essential for the characteristic association of the complex with chromatin.

The PWWP domain is necessary for chromatin association of Brpf1

Bromodomains are known to mediate binding to acetylated histones (Yang, 2004), and PHD fingers to methylated histone residues (Pena et al., 2006; Wysocka et al., 2006). Brpf1 contains a PHD finger, a bromodomain, and a C-terminal PWWP domain, for which histone-binding capacity had not yet been reported. To dissect which domains of Brpf1 mediate chromatin association, we determined the localization of different truncated versions of Brpf1 in cells (Fig. 6H). Full-length Brpf1 localized to distinct sites of condensed chromosomes (Fig. 6A,B). Strikingly, deletion of the C-terminal PWWP domain led to a total exclusion of Brpf1 from condensed chromosomes (Fig. 6, compare C with B). The same exclusion was obtained for a Brpf1 fragment consisting only of the PHD finger and bromodomain (Fig. 6D). By contrast, a fusion of the PWWP domain and bromodomain restored the typical association with mitotic chromosomes (Fig. 6E) and the co-localization with active histone marks (Fig. 6, compare L with I), whereas neither the PWWP domain nor bromodomain was alone sufficient for proper localization (data not shown). PWWP domain-dependent chromatin localization during both interphase and metaphase was also observed for GFP-Brpf1 in zebrafish embryos (see Fig. S7 in the supplementary material). Together, these data indicate that the PWWP domain is absolutely essential and, together with the bromodomain, sufficient for chromatin targeting of Brpf1, whereas the PHD and zinc-finger domains are dispensable. Interestingly, in contrast to interphase (Fig. 5A), Brpf1 and Moz did not co-localize during mitosis, when Moz was largely excluded from chromosomes (Fig. 6F,G; see Discussion).

The PWWP of Brpf1 directly binds histones

To study whether the PWWP- and bromodomain-dependent chromatin association of Brpf1 is mediated by direct binding to histones, we generated recombinant GST fusions of the PHD finger, the bromodomain and the PWWP domain (Fig. 7A), and performed affinity purifications with human core histones. In these assays, the bromodomain bound the four core histones equally, the PWWP domain displayed stronger and preferential binding to H2B and H2A, and the PHD domain no binding at all (Fig. 7B). Furthermore, the PWWP domain bound efficiently to purified calf thymus H2A or H2B, whereas no, or less, binding was observed for the bromodomain (Fig. 7C). This suggests that the PWWP domain can directly bind H2A and H2B, whereas the bromodomain might require H3 and H4 or histone octamers. Furthermore, affinity purifications and subsequent western blot analyses with normal or hyperacetylated histones revealed that the bromodomain binds preferentially to acetylated H2A, whereas no such preference was detected for the PWWP domain (Fig. 7D; compare lanes 3, 4 with 5, 6 and 7, 8), suggesting that the PWWP domain can bind H2 histones independently of their acetylation status.

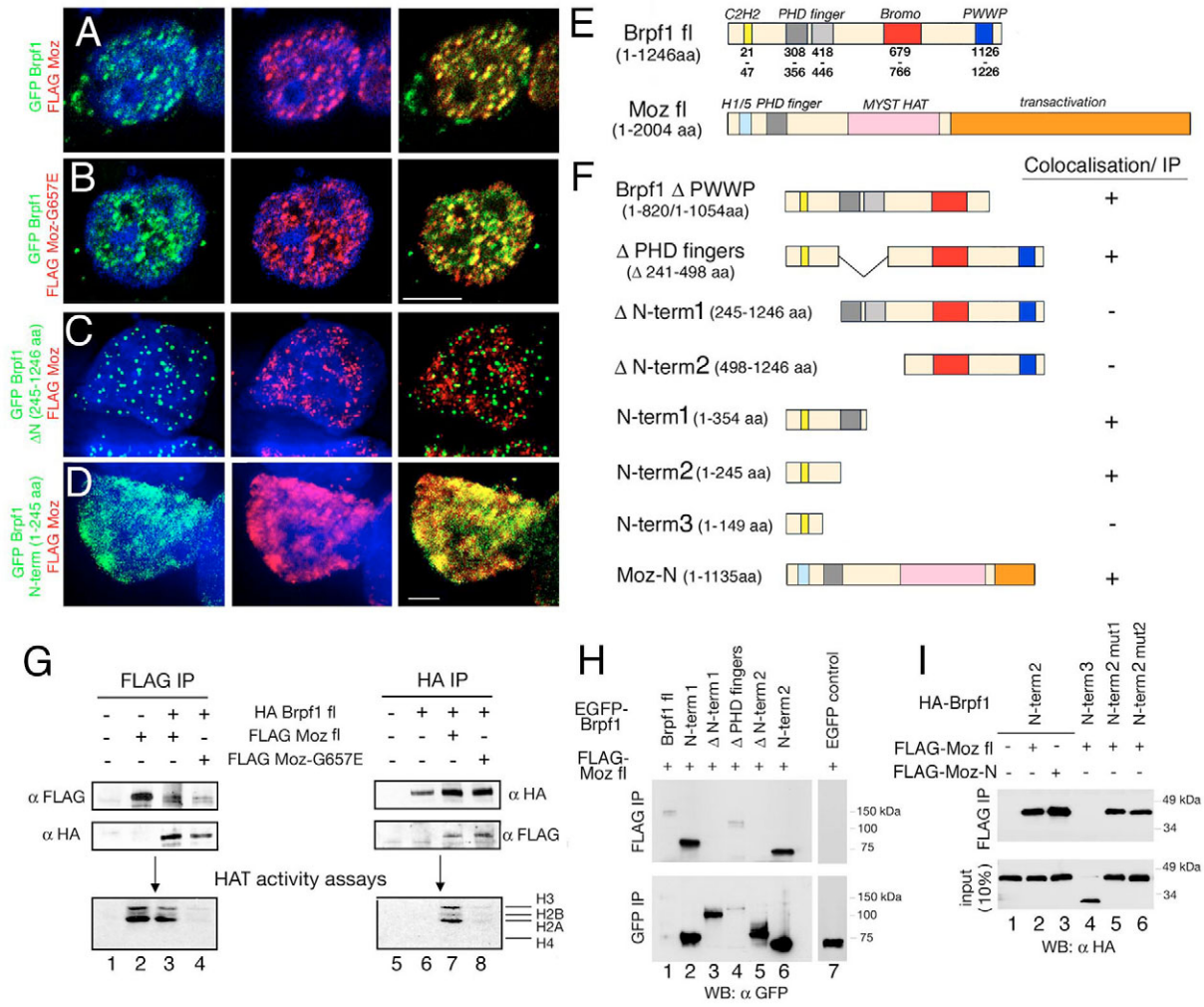

Fig. 5. Co-localization and physical interaction of Brpf1 and Moz. (**A-D**) Brpf1 co-localizes with Moz. Immunofluorescent staining of interphase HEK 293 cells after co-transfection with the indicated versions of GFP-Brpf1 (left panels; green) and FLAG-Moz (middle panels; red), counterstained with DAPI (for DNA; blue); merged images are shown in right-hand panels. Full-length Brpf1 co-localizes with wild-type Moz (A) and with HAT-negative Moz-G675E (B) in a punctate pattern on interphase nuclei. Co-localization is abolished when Brpf1 is N-terminally truncated (C). N-terminal fragment of Brpf1 co-localizes with Moz, but displays a more diffuse distribution (D). (**E**,**F**) Schematic structures and co-localization/immunoprecipitation properties of full-length Brpf1, full-length Moz (E), and the various truncations used (F). (**G-I**) Brpf1 physically associates with Moz. (G) Co-IP of full-length Brpf1 and wild-type or HAT-negative Moz(G657E) from co-transfected cells with anti-FLAG (Moz) antibody (left) or anti-HA (Brpf1) antibody (right), analyzed in western blots (upper panels) with the specified antibodies, or assayed for HAT activity on core histones (lower panels). (H) Co-IP of full-length FLAG-Moz and various GFP-Brpf1 deletion constructs with anti-FLAG or anti-GFP antibodies, followed by analysis of complex formation (upper panel) and control for Brpf1 expression levels (lower panel) via anti-GFP western blotting. (I) Co-IP of full-length Moz or C-terminally truncated MozN and various HA-tagged versions of the N-terminal fragments of Brpf1 using anti-FLAG antibody, analyzed in anti-HA western blots. Lower panel shows input control. Brpf1 aa 1-245 fragments that have histidine or cysteine mutations in the zinc-finger domain can still co-precipitate with Moz (lanes 5, 6), whereas the aa 1-149 fragment with an intact zinc finger cannot (lane 4). Scale bars: 5 μm in B; 2.5 μm in D.

DISCUSSION

Zebrafish Brpf1 is required for maintenance of Hox gene expression and pharyngeal segmental identity

Despite its identification almost 15 years ago, there had been little information about the role of Brpf1 in vertebrate systems. Here, we have studied both its biological and molecular function, applying a combination of loss-of-function studies in zebrafish with protein localization and biochemical analyses.

Zebrafish mutants lacking zygotic Brpf1 display progressively reduced expression of anterior Hox genes in CNC cells, which in turn causes anterior shifts in segmental identity of pharyngeal arches 2-6. The complexity of the craniofacial phenotype, which is very similar to that of *moz* mutants (Miller et al., 2004), is most likely due to misregulation of multiple Hox genes. *hox2* acts as a selector gene for second arch segmental identity, and mutation of *Hoxa2* in mouse or reduction of *hoxa2b* and *hoxb2a* function in zebrafish results in a homeotic transformation of second to first arch identity (Gendron-Maguire et al., 1993; Hunter and Prince, 2002; Rijli et al., 1993). In this light, the bimandibular phenotype of *brpf1* mutants can be explained by the requirement of Brpf1 for maintained *hoxa2b* and *hoxb2a* expression. Similarly, the acquirement of second arch characteristics in arches 3-6 of *brpf1* mutants might result from its role in *hoxb3a* expression, consistent

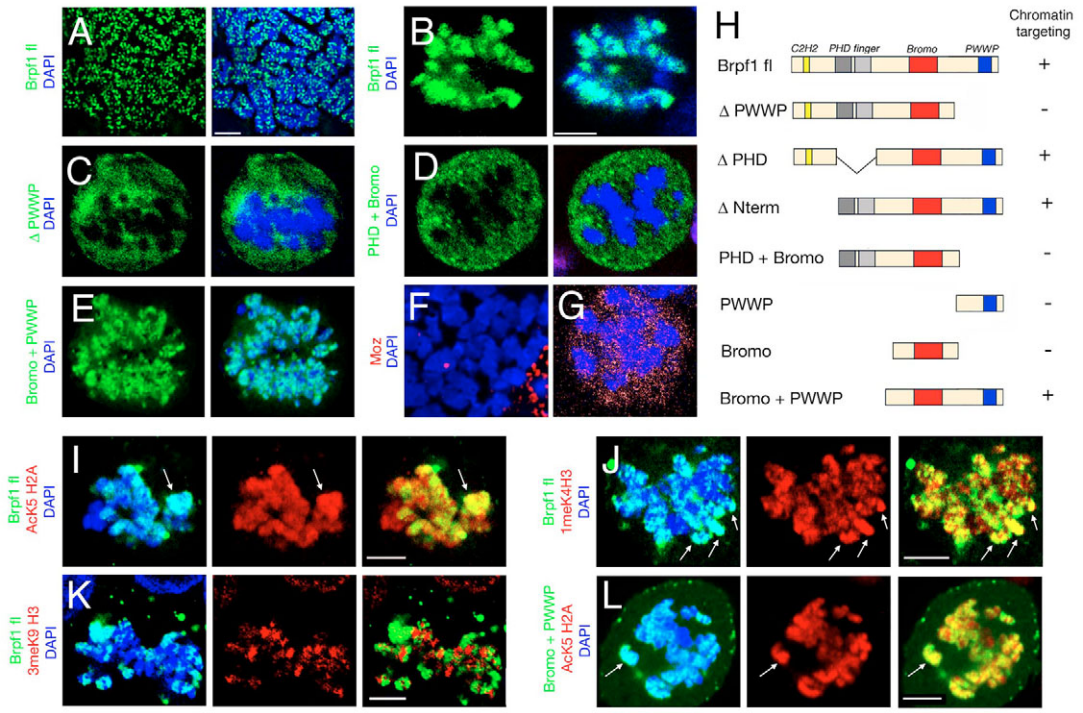

Fig. 6. The PWWP domain is required for association of Brpf1 with metaphase chromosomes. (**A-G**) Immunofluorescent staining of mitotic HEK 293 cells transfected with the indicated GFP-Brpf1 constructs (A-E; green) and FLAG-Moz (F,G; red). (A,F) Spreads of metaphase chromosomes. Right panels of A-E and F,G show merged images with DAPI staining of DNA (blue). Full-length Brpf1 displays punctate distribution along metaphase chromosomes (A), whereas in intact nuclei, localization is concentrated in fewer, but still distinct domains of the DNA (B). Truncated Brpf1 lacking the PWWP domain (C) and a Brpf1 fragment containing the PHD domain and the bromodomain (D) are excluded from mitotic chromosomes, whereas a Brpf1 fragment containing the bromodomain and the PWWP domain co-localizes with DNA (E) in a similar manner to full-length Brpf1 (B). (F,G) In contrast to Brpf1 (A,B), no chromatin association is apparent for Moz in metaphase chromosome spreads (F) and in intact mitotic nuclei (G). (**H**) Schematic structures and chromosome-targeting properties of the full-length and truncated versions of Brpf1. (**I-L**) Immunofluorescent staining of mitotic HEK 293 cells, revealing that full-length Brpf1 (I-K; green) and the fragment containing the bromodomain and PWWP domain (L; green) co-localize with the active chromatin markers H2AK5Ac (I,L; red) and H3K4me1 (J; red), but not with the inactive chromatin marker H3K9me3 (K; red). Left panels are counterstained with DAPI (blue); merged images are shown in right-hand panels; regions with strong co-localization (yellow) are indicated by arrows. Scale bars: 2.5 μm in A; 5 μm in B,I-L.

with data obtained in mouse reporting that loss of Hoxa3 function leads to disruptions in the formation of third pouch derivatives (Manley and Capecchi, 1995).

During normal development, *brpf1* is not only expressed in CNC that forms the pharyngeal arch cartilage, but also in pharyngeal ectoderm and endoderm. Previous studies have indicated that Hox gene expression in premigratory CNC cells does not irreversibly determine their segmental identity. Rather, migrating CNC cells receive additional instructive information from surrounding tissues (see Crump et al., 2004a; Piotrowski and Nüsslein-Volhard, 2000; Trainor and Krumlauf, 2000). However, our grafting experiments show that Brpf1 function in the endoderm is dispensable for pharyngeal segmental identity, whereas its effect on Hox gene expression in the CNC is cell-autonomous. This suggests that for the determination of arch identity, Brpf1 is exclusively required in the CNC, as has also recently been shown for its interaction partner Moz (Crump et al., 2006). Future experiments will need to show whether the same is true for arch-associated dermal bones, which are most likely also CNC derivatives that show corresponding transformations in *brpf1* mutants. By contrast, the anterior shifts in facial muscular organization seem to be secondary consequences of the cartilage transformations, as the earlier pattern of muscle progenitor cells appears normal (K.L. and M.H., unpublished).

Brpf1 behaves like a TrxG member

TrxG and PcG proteins are key regulators of chromatin structure (Ringrose and Paro, 2004; Ringrose and Paro, 2007). Several lines of evidence suggest that Brpf1 is a novel TrxG member. First, it is required for maintenance, but not initiation, of Hox gene expression, a hallmark of TrxG mutants in flies (Breen and Harte, 1993) and mouse (Yu et al., 1998). Second, it genetically interacts and physically associates with a HAT, and defects of *brpf1* mutants can be rescued by inhibition of HDAC activity, consistent with the HAT association and HDAC sensitivity of many TrxG factors and mutations (Milne et al., 2002; Petruk et al., 2001). Third, Brpf1 contains a combination of domains found in other TrxG proteins (bromo, PWWP, PHD finger, zinc finger, AT hooks) (Ringrose and Paro, 2004). Fourth, it directly binds histones, as do several TrxG proteins containing bromodomains and/or chromo/PHD-finger domains (Ringrose and Paro, 2004; Yang, 2004). Fifth, Brpf1 co-localizes with histone modifications enriched in active chromatin.

TrxG proteins are supposed to keep genes active throughout the cell cycle. During mitosis, there is a global shutdown of transcription, and genes remain silent unless they have been marked during the previous interphase (Ringrose and Paro, 2007). In the *Drosophila* genome, TrxG-mediated marking for

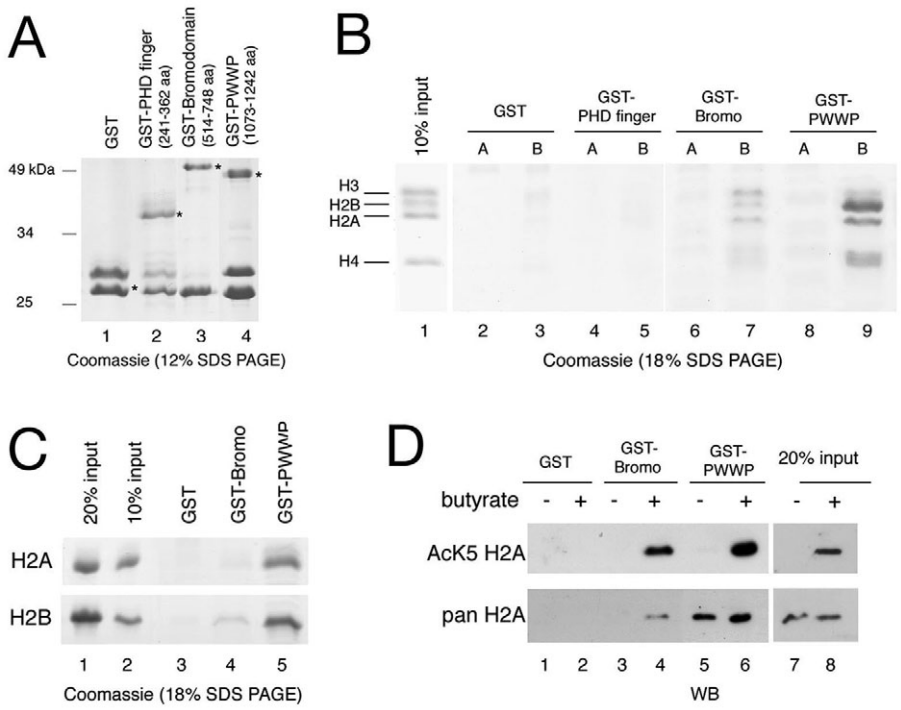

Fig. 7. The bromodomain and PWWP domain bind histones. (**A**) Loading controls of GST-fused recombinant domains of Brpf1 (PHD finger, bromodomain, or PWWP domain) used in histone-binding assays (B-D). Relevant bands are indicated with asterisks. (**B**) Coomassie-staining of histones retained on glutathion beads without (A) or with (B) indicated GST-Brpf1 domains. Left lane shows 10% input of core histones used per assay. (**C**) Binding of purified H2A or H2B from calf serum with indicated GST-Brpf1 domains, analyzed by Coomassie staining. (**D**) Binding of core histones from untreated or butyrate-treated HeLa cells with indicated GST-Brpf1 domains, analyzed by western blotting with anti-H2AK5Ac (upper panel) or anti-H2A (lower panel) antibodies. The PWWP domain binds regular and hyperacetylated H2A equally well (compare lanes 5 and 6 of lower panel), whereas the bromodomain preferentially binds hyperacetylated H2A (compare lanes 3 and 4 of lower panel). This is also reflected in the higher relative signal intensity obtained with the anti-H2AK5Ac and the anti-pan H2A antibodies (compare upper and lower bands of lane 4 with those of lanes 6 and 8).

transcriptional reinitiation occurs at PRE/TREs, and corresponding sites, although not yet identified at the molecular level, have been suggested to exist in vertebrates (Ringrose and Paro, 2007). Interestingly, we found Brpf1 to be associated with chromatin in discrete spots in both interphase and mitotic chromosomes of HEK 293 cells and zebrafish embryos. Thus, it is tempting to speculate that Brpf1 might account for this TrxG-mediated transcriptional memory through mitosis and cell division. Interestingly, Moz, although co-localized with Brpf1 during interphase, is not retained on mitotic chromosomes, suggesting that only a specific sub-complex is involved in the physical marking of certain genes during mitosis.

Molecular mechanisms of Brpf1 function and the roles of its multiple domains

To understand the molecular mechanisms of Brpf1 function, we carried out a series of studies comparing the properties of full-length Brpf1 protein with those of various truncated or mutant versions. We found that Brpf1 physically associates with the HAT Moz, which extends previous findings (Doyon et al., 2006) and is consistent with our immunofluorescence and genetic data, which indicate that Brpf1 is required for proper chromatin localization and in vivo function of Moz. We mapped the Moz-interaction domain in Brpf1 to thus far uncharacterized motifs between aa 150 and 245. However, it remains unclear whether the binding is direct or indirect, being mediated by other proteins such as Ing5 (Doyon et al., 2006). In addition, we showed that both the bromodomain (aa 679-766) and the PWWP domain (aa 1126-1226) are involved in chromatin binding of Brpf1. A combination of both domains localized to active chromatin, whereas the individual domains and truncated Brpf1 lacking the PWWP domain did not, pointing to an essential cooperative function of the two domains, as has recently been described for bromo-PHD modules in other proteins (Pena et al., 2006; Wysocka et al., 2006). Consistent with this, the bromodomain and the PWWP domain were found to bind histones with different specificities. The bromodomain showed a significant preference for acetylated histones, as does this domain in other proteins (Yang, 2004), whereas the PWWP domain did not. Conversely, PWWP showed a preference for histones H2A and H2B, whereas the bromodomain bound all core histones equally. Our findings are the first demonstration of direct histone binding for a PWWP domain. This puts PWWP domains on a par with the structurally related and well-known histone-binding chromo and MBT domains (Maurer-Stroh et al., 2003). The importance of this binding is highlighted by the fact that zebrafish mutants lacking only the PWWP domain displayed the *brpf1*-null phenotype, demonstrating that it is absolutely essential for Brpf1 function in vivo. Future experiments will need to show whether the Brpf1 PWWP domain has any preference for other histone modifications. Interestingly, histone binding of Brpf1 also seems to be required for proper localization of Moz on interphase chromatin. Although Moz has previously been reported to be able to bind nucleosomes (Deguchi et al., 2003), we found its nuclear distribution upon co-transfection with the N-terminal fragment of Brpf1 to be rather diffuse, in contrast to its localization at discrete sites upon co-transfection with full-length Brpf1.

In summary, our data propose a model in which Brpf1, as conferred by its unique set of domains, acts in multiple steps to keep Hox and possibly other genes active during vertebrate development. Mediated by its PWWP domain, it can bind to H2A/H2B histones independently of their acetylation status, and remains at discrete genomic loci even during mitosis, marking them for reinitiation of activation. After mitosis, and mediated by its N-terminal domain, it recruits Moz to chromatin, triggering acetylation of histones H3 and H2A (the latter of which had not previously been identified as a Moz substrate). Finally, mediated by binding of its bromodomain to acetylated histones, Brpf1 protects histones from deacetylation by HDACs.

We thank the Consortium of the Tübingen 2000 screen, during which the *brpf1 t20002* and *25114* alleles were isolated, and V. Prince, L. Zon, C. Miller, M. Ekker and D. Heery for providing plasmids. Work in M.H.'s laboratory was supported by the European Union (6th framework), work in R.S.'s laboratory by HFSPO (Career Development Award), the Epigenome Network of Excellence and the DFG (SFB756).

Tübingen 2000 Screen Consortium
F. van Bebber, E. Busch-Nentwich, R. Dahm, H. G. Frohnhöfer, H. Geiger, D. Gilmour, S. Holley, J. Hooge, D. Jülich, H. Knaut, F. Maderspacher, H.-M. Maischein, C. Neumann, T. Nicolson, C. Nüsslein-Volhard, H. H. Roehl, U. Schönberger, C. Seiler, C. Söllner, M. Sonawane and A. Wehner at the Max-Planck Institute of Developmental Biology, Spemannstrasse 35, D-72076 Tübingen, Germany.

P. Erker, H. Habeck, U. Hagner, C. Hennen, E. Kaps, A. Kirchner, T. Koblitzek, U. Langheinrich, C. Loeschke, C. Metzger, R. Nordin, J. Odenthal, M. Pezzuti, K. Schlombs, J. deSatana-Stamm, T. Trowe, G. Vacun, B. Walderich, A. Walker and C. Weiler at Artemis Pharmaceuticals, Spemannstrasse 35, D-72076 Tübingen, Germany.

Supplementary material
Supplementary material for this article is available at
http://dev.biologists.org/cgi/content/full/135/11/1935/DC1

References

Akimenko, M.-A., Ekker, M., Wegner, J., Lin, W. and Westerfield, M. (1994). Combinatorial expression of three zebrafish genes related to *distal-less*: part of a homeobox gene code for the head. *J. Neurosci.* **16**, 3475-3486.
Bannister, A. J. and Kouzarides, T. (1996). The CBP co-activator is a histone acetyltransferase. *Nature* **384**, 641-643.
Breen, T. R. and Harte, P. J. (1993). Trithorax regulates multiple homeotic genes in the bithorax and Antennapedia complexes and exerts different tissue-specific, parasegment-specific and promoter-specific effects on each. *Development* **117**, 119-134.
Carney, T. J., von der Hardt, S., Sonntag, C., Amsterdam, A., Topczewski, J., Hopkins, N. and Hammerschmidt, M. (2007). Inactivation of serine protease Matriptase1a by its inhibitor Hai1 is required for epithelial integrity of the zebrafish epidermis. *Development* **134**, 3461-3471.
Collins, H. M., Kindle, K. B., Matsuda, S., Ryan, C., Troke, P. J., Kalkhoven, E. and Heery, D. M. (2006). MOZ-TIF2 alters cofactor recruitment and histone modification at the RARbeta2 promoter: differential effects of MOZ fusion proteins on CBP- and MOZ-dependent activators. *J. Biol. Chem.* **281**, 17124-17133.
Crump, J. G., Swartz, M. E. and Kimmel, C. B. (2004a). An integrin-dependent role of pouch endoderm in hyoid cartilage development. *PLoS Biol.* **2**, E244.
Crump, J. G., Maves, L., Lawson, N. D., Weinstein, B. M. and Kimmel, C. B. (2004b). An essential role for FGFs in endodermal pouch formation influences later craniofacial skeletal patterning. *Development* **131**, 5703-5716.
Crump, J. G., Swartz, M. E., Eberhart, J. K. and Kimmel, C. B. (2006). Moz-dependent Hox expression controls segment-specific fate maps of skeletal precursors in the face. *Development* **133**, 2661-2669.
Deguchi, K., Ayton, P. M., Carapeti, M., Kutok, J. L., Snyder, C. S., Williams, I. R., Cross, N. C., Glass, C. K., Cleary, M. L. and Gilliland, D. G. (2003). MOZ-TIF2-induced acute myeloid leukemia requires the MOZ nucleosome binding motif and TIF2-mediated recruitment of CBP. *Cancer Cell* **3**, 259-271.
Doyon, Y., Cayrou, C., Ullah, M., Landry, A. J., Cote, V., Selleck, W., Lane, W. S., Tan, S., Yang, X. J. and Cote, J. (2006). ING tumor suppressor proteins are critical regulators of chromatin acetylation required for genome expression and perpetuation. *Mol. Cell* **21**, 51-64.
Geisler, R. (2002). Mapping and cloning. In *Zebrafish: A Practical Approach*. Vol. 261 (ed. C. Nüsslein-Volhard and R. Dahm), pp. 175-212. Oxford: Oxford University Press.
Gendron-Maguire, M., Mallo, M., Zhang, M. and Gridley, T. (1993). Hoxa-2 mutant mice exhibit homeotic transformation of skeletal elements derived from cranial neural crest. *Cell* **75**, 1317-1331.
Grammatopoulos, G. A., Bell, E., Toole, L., Lumsden, A. and Tucker, A. S. (2000). Homeotic transformation of branchial arch identity after Hoxa2 overexpression. *Development* **127**, 5355-5365.
Hammerschmidt, M., Pelegri, F., Mullins, M. C., Kane, D. A., van Eeden, F. J., Granato, M., Brand, M., Furutani-Seiki, M., Haffter, P., Heisenberg, C. P. et al. (1996). dino and mercedes, two genes regulating dorsal development in the zebrafish embryo. *Development* **123**, 95-102.
Hauptmann, G. and Gerster, T. (1994). Two-color whole-mount in situ hybridization to vertebrate and Drosophila embryos. *Trends Genet.* **10**, 266.
Hunt, P., Gulisano, M., Cook, M., Sham, M. H., Faiella, A. Wilkinson, D., Boncinelli, E. and Krumlauf, R. (1991). A distinct Hox code for the branchial region of the vertebrate head. *Nature* **353**, 861-844.
Hunter, M. P. and Prince, V. E. (2002). Zebrafish hox paralogue group 2 genes function redundantly as selector genes to pattern the second pharyngeal arch. *Dev. Biol.* **247**, 367-389.
Isogai, S., Lawson, N. D., Torrealday, S., Horiguchi, M. and Weinstein, B. M. (2003). Angiogenic network formation in the developing vertebrate trunk. *Development* **130**, 5281-5290.
Katsumoto, T., Aikawa, Y., Iwama, A., Ueda, S., Ichikawa, H., Ochiya, T. and Kitabayashi, I. (2006). MOZ is essential for maintenance of hematopoietic stem cells. *Genes Dev.* **20**, 1321-1330.
Keohane, A. M., O'Neill, L, P., Belyaev, N. D., Lavender, J. S. and Turner, B. M. (1996). X-Inactivation and histone H4 acetylation in embryonic stem cells. *Dev. Biol.* **180**, 618-630.
Le Douarin, N. M. (1982). *The Neural Crest*. Cambridge: Cambridge University Press.
Manley, N. R. and Capecchi, M. R. (1995). The role of Hoxa-3 in mouse thymus and thyroid development. *Development* **121**, 1989-2003.
Maurer-Stroh, S., Dickens, N. J., Hughes-Davies, L., Kouzarides, T., Eisenhaber, F. and Ponting, C. P. (2003). The Tudor domain 'Royal Family': Tudor, plant Agenet, Chromo, PWWP and MBT domains. *Trends Biochem. Sci.* **28**, 69-74.
McClintock, J. M., Carlson, R., Mann, D. M. and Prince, V. E. (2001). Consequences of Hox gene duplication in the vertebrates: an investigation of the zebrafish Hox paralogue group 1 genes. *Development* **128**, 2471-2484.
Miller, C. T., Yelon, D., Stainier, D. Y. and Kimmel, C. B. (2003). Two endothelin 1 effectors, hand2 and bapx1, pattern ventral pharyngeal cartilage and the jaw joint. *Development* **130**, 1353-1365.
Miller, C. T., Maves, L. and Kimmel, C. B. (2004). moz regulates Hox expression and pharyngeal segmental identity in zebrafish. *Development* **131**, 2443-2461.
Milne, T. A., Briggs, S. D., Brock, H. W., Martin, M. E., Gibbs, D., Allis, C. D. and Hess, J. L. (2002). MLL targets SET domain methyltransferase activity to Hox gene promoters. *Mol. Cell* **10**, 1107-1117.
Nornes, S., Mikkola, I., Krauss, S., Delghandi, M., Perander, M. and Johansen, T. (1996). Zebrafish Pax9 encodes two proteins with distinct C-terminal transactivating domains of different potency negatively regulated by adjacent N-terminal sequences. *J. Biol. Chem.* **271**, 26914-26923.
Okabe, M. and Graham, A. (2004). The origin of the parathyroid gland. *Proc. Natl. Acad. Sci. USA* **101**, 17716-17719.
Pasqualetti, M., Ori, M., Nardi, I. and Rijli, F. M. (2000). Ectopic Hoxa2 induction after neural crest migration results in homeosis of jaw elements in Xenopus. *Development* **127**, 5367-5378.
Pena, P. V., Davrazou, F., Shi, X., Walter, K. L., Verkhusha, V. V., Gozani, O., Zhao, R. and Kutateladze, T. G. (2006). Molecular mechanism of histone H3K4me3 recognition by plant homeodomain of ING2. *Nature* **442**, 100-103.
Petruk, S., Sedkov, Y., Smith, S., Tillib, S., Kraevski, V., Nakamura, T., Canaani, E., Croce, C. M. and Mazo, A. (2001). Trithorax and dCBP acting in a complex to maintain expression of a homeotic gene. *Science* **294**, 1331-1334.
Piotrowski, T. and Nüsslein-Volhard, C. (2000). The endoderm plays an important role in patterning the segmented pharyngeal region in zebrafish (Danio rerio). *Dev. Biol.* **225**, 339-356.
Popovic, R. and Zeleznik-Le, N. J. (2005). MLL: how complex does it get? *J. Cell. Biochem.* **95**, 234-242.
Rijli, F. M., Mark, M., Lakkaraju, S., Dierich, A., Dolle, P. and Chambon, P. (1993). A homeotic transformation is generated in the rostral branchial region of the head by disruption of Hoxa-2, which acts as a selector gene. *Cell* **75**, 1333-1349.
Ringrose, L. and Paro, R. (2004). Epigenetic regulation of cellular memory by the Polycomb and Trithorax group proteins. *Annu. Rev. Genet.* **38**, 413-443.
Ringrose, L. and Paro, R. (2007). Polycomb/Trithorax response elements and epigenetic memory of cell identity. *Development* **134**, 223-232.
Santagati, F. and Rijli, F. M. (2003). Cranial neural crest and the building of the vertebrate head. *Nat. Rev. Neurosci.* **4**, 806-818.
Santagati, F., Minoux, M., Ren, S. Y. and Rijli, F. M. (2005). Temporal requirement of Hoxa2 in cranial neural crest skeletal morphogenesis. *Development* **132**, 4927-4936.
Shi, X., Hong, T., Walter, K. L., Ewalt, M., Michishita, E., Hung, T., Carney, D., Pena, P., Lan, F., Kaadige, M. R. et al. (2006). ING2 PHD domain links histone H3 lysine 4 methylation to active gene repression. *Nature* **442**, 96-99.
Simon, J. A. and Tamkun, J. W. (2002). Programming off and on states in chromatin: mechanisms of Polycomb and trithorax group complexes. *Curr. Opin. Genet. Dev.* **12**, 210-218.
Thomas, T., Corcoran, L. M., Gugasyan, R., Dixon, M. P., Brodnicki, T., Nutt, S. L., Metcalf, D. and Voss, A. K. (2006). Monocytic leukemia zinc finger

protein is essential for the development of long-term reconstituting hematopoietic stem cells. *Genes Dev.* **20**, 1175-1186.
Thompson, K. A., Wang, B., Argraves, W. S., Giancotti, F. G., Schranck, D. P. and Ruoslahti, E. (1994). BR140, a novel zinc-finger protein with homology to the TAF250 subunit of TFIID. *Biochem. Biophys. Res. Commun.* **198**, 1143-1152.
Trainor, P. and Krumlauf, R. (2000). Plasticity in mouse neural crest cells reveals a new patterning role for cranial mesoderm. *Nat. Cell Biol.* **2**, 96-102.
Van der Heyden, C., Wautier, K. and Huysseune, A. (2001). Tooth succession in the zebrafish (Danio rerio). *Arch. Oral Biol.* **46**, 1051-1058.
Walker, M. B. and Kimmel, C. B. (2007). A two-color acid-free cartilage and bone stain for zebrafish larvae. *Biotech. Histochem.* **82**, 23-28.
Wysocka, J., Swigut, T., Xiao, H., Milne, T. A., Kwon, S. Y., Landry, J., Kauer, M., Tackett, A. J., Chait, B. T., Badenhorst, P. et al. (2006). A PHD finger of NURF couples histone H3 lysine 4 trimethylation with chromatin remodelling. *Nature* **442**, 86-90.
Yagi, H., Deguchi, K., Aono, A., Tani, Y., Kishimoto, T. and Komori, T. (1998). Growth disturbance in fetal liver hematopoiesis of Mll-mutant mice. *Blood* **92**, 108-117.
Yan, Y. L., Miller, C. T., Nissen, R. M., Singer, A., Liu, D., Kirn, A., Draper, B., Willoughby, J., Morcos, P. A., Amsterdam, A. et al. (2002). A zebrafish sox9 gene required for cartilage morphogenesis. *Development* **129**, 5065-5079.
Yang, X. J. (2004). Lysine acetylation and the bromodomain: a new partnership for signaling. *BioEssays* **26**, 1076-1087.
Yu, B. D., Hess, J. L., Horning, S. E., Brown, G. A. and Korsmeyer, S. J. (1995). Altered Hox expression and segmental identity in Mll-mutant mice. *Nature* **378**, 505-508.
Yu, B. D., Hanson, R. D., Hess, J. L., Horning, S. E. and Korsmeyer, S. J. (1998). MLL, a mammalian trithorax-group gene, functions as a transcriptional maintenance factor in morphogenesis. *Proc. Natl. Acad. Sci. USA* **95**, 10632-10636.